### Title

Ischaemic preconditioning preferentially increases protein S-nitrosylation in subsarcolemmal mitochondria




### Journal

Cardiovascular Research, 106(2)

### ISSN

1015-5007



### Authors

Sun, Junhui
Nguyen, Tiffany
Aponte, Angel M
et al.



### Publication Date

2015-05-01

### DOI

10.1093/cvr/cvv044

Peer reviewed

Cardiovascular Research (2015) **106**, 227–236
doi:10.1093/cvr/cvv044

# Ischaemic preconditioning preferentially increases protein S-nitrosylation in subsarcolemmal mitochondria

**Junhui Sun[1]*, Tiffany Nguyen[1], Angel M. Aponte[1,2], Sara Menazza[1], Mark J. Kohr[1,3], David M. Roth[4], Hemal H. Patel[4], Elizabeth Murphy[1], and Charles Steenbergen[3]**

[1]Systems Biology Center, National Heart Lung and Blood Institute, National Institutes of Health, 10 Center Drive, Bldg10/Rm8N206, Bethesda, MD 20892, USA; [2]Proteomics Core Facility, National Heart Lung and Blood Institute, National Institutes of Health, Bethesda, MD 20892, USA; [3]Department of Pathology, Johns Hopkins Medical Institutions, Baltimore, MD 21205, USA; and [4]Department of Anesthesiology, VA San Diego Healthcare System and University of California at San Diego, La Jolla, CA 92093, USA

*Received 17 December 2014; revised 4 February 2015; accepted 8 February 2015; online publish-ahead-of-print 18 February 2015*

**Time for primary review: 35 days**

Nitric oxide (NO) and protein S-nitrosylation (SNO) have been shown to play important roles in ischaemic preconditioning (IPC)-induced acute cardioprotection. The majority of proteins that show increased SNO following IPC are localized to the mitochondria, and our recent studies suggest that caveolae transduce acute NO/SNO cardioprotective signalling in IPC hearts. Due to the close association between subsarcolemmal mitochondria (SSM) and the sarcolemma/caveolae, we tested the hypothesis that SSM, rather than the interfibrillar mitochondria (IFM), are major targets for NO/SNO signalling derived from caveolae-associated eNOS. Following either control perfusion or IPC, SSM and IFM were isolated from Langendorff perfused mouse hearts, and SNO was analysed using a modified biotin switch method with fluorescent maleimide fluors. In perfusion control hearts, the SNO content was higher in SSM compared with IFM (1.33 $\pm$ 0.19, ratio of SNO content Perf-SSM vs. Perf-IFM), and following IPC SNO content significantly increased preferentially in SSM, but not in IFM (1.72 $\pm$ 0.17 and 1.07 $\pm$ 0.04, ratio of SNO content IPC-SSM vs. Perf-IFM, and IPC-IFM vs. Perf-IFM, respectively). Consistent with these findings, eNOS, caveolin-3, and connexin-43 were detected in SSM, but not in IFM, and IPC resulted in a further significant increase in eNOS/caveolin-3 levels in SSM. Interestingly, we did not observe an IPC-induced increase in SNO or eNOS/caveolin-3 in SSM isolated from caveolin-3$^{-/-}$ mouse hearts, which could not be protected with IPC. In conclusion, these results suggest that SSM may be the preferential target of sarcolemmal signalling-derived post-translational protein modification (caveolae-derived eNOS/NO/SNO), thus providing an important role in IPC-induced cardioprotection.

**Keywords** Protein S-nitrosylation • Ischaemic preconditioning • Caveolae • Subsarcolemmal and interfibrillar mitochondria

## 1. Introduction

Mitochondria play a central role in cell death and survival and have been suggested to be the end effector of cardioprotective interventions, such as ischaemic preconditioning (IPC) and postconditioning (PostC).[1,2] Although, IPC has been shown to depend on G-protein coupled receptor signalling, the details of the mechanism by which these signals are transduced to the mitochondria requires further study. Caveolae-mediated endocytosis has been suggested to result in the formation of a signalosome, which is thought to target mitochondria and may be G-protein sensitive.[3–6] Caveolae have been found to play an essential role in IPC-induced cardioprotection, since the disruption of caveolae, either by pharmacological treatment with cholesterol sequestering agent[7,8] or genetic deletion of the marker protein caveolin-3,[7] abolishes IPC-induced protection. Conversely, cardiac-specific overexpression of caveolin-3 has been found to induce endogenous cardioprotection by mimicking IPC.[9,10]

In cardiomyocytes, multiple signalling molecules are concentrated and organized within the caveolae to mediate signal transduction.[11,12] Endothelial nitric oxide synthase (eNOS) and its product nitric oxide (NO) have been reported to play important cardioprotective roles in ischaemia–reperfusion (I/R) injury,[13,14] although the role of endogenous NO in I/R and IPC remains controversial.[15–19] Besides activating the sGC/cGMP signalling pathways, NO can directly modify protein sulfhydryl residues through protein S-nitrosylation (SNO), which has emerged as an important post-translational protein modification in cardiovascular signalling[20,21] and cardioprotection.[22,23] In our recent studies, we found that IPC leads to the association of caveolin-3 and eNOS with the mitochondria, and this results in increased mitochondrial protein SNO.[8] Interestingly, disruption of caveolae via cholesterol sequestering

* Corresponding author: Tel: +1 301 496 8192; fax: +1 301 402 0190, Email: sun1@mail.nih.gov

agents (i.e. methyl-β-cyclodextrin), abolished the mitochondrial association of eNOS, and blocked the increase in SNO and cardioprotection afforded by IPC.[8]

There are two distinct populations of mitochondria that are distributed in cardiomyocytes according to their subcellular localization. Subsarcolemmal mitochondria (SSM) are located directly beneath the sarcolemma, while interfibrillar mitochondria (IFM) are aligned among the myofibrils.[24,25] Given the close proximity of SSM to caveolae and the sarcolemma, it is possible that caveolae-mediated cardioprotective signalling may preferentially target SSM, rather than IFM. Therefore, the goal of this study was to test whether SSM, rather than IFM, are the major targets for caveolae-derived eNOS/NO/SNO signalling.

# 2. Methods

## 2.1 Animals

C57BL/6J wild-type (WT) male mice were obtained from Jackson Laboratories (Bar Harbor, ME, USA) and caveolin-3$^{-/-}$ male mice were provided by Drs Hemal Patel and David Roth (Department of Anesthesiology, University of California at San Diego). Mice were 10–12 weeks of age at the time of experimentation. All animals were treated in accordance with National Institutes of Health guidelines and the 'Guiding Principles for Research Involving Animals and Human Beings'. This study was reviewed and approved by the Institutional Animal Care and Use Committee of the National Heart Lung and Blood Institute.

## 2.2 Langendorff heart perfusion and IPC protocol

Mice were anaesthetized with pentobarbital (50 mg/kg) and anti-coagulated with heparin. Hearts were excised quickly and placed in ice-cold Krebs–Henseleit buffer (in mmol/L: 120 NaCl, 11 D-glucose, 25 $NaHCO_3$, 1.75 $CaCl_2$, 4.7 KCl, 1.2 $MgSO_4$, and 1.2 $KH_2PO_4$). The aorta was cannulated on a Langendorff apparatus and the heart was perfused in retrograde fashion with Krebs–Henseleit buffer at a constant pressure of 100 cm of water at 37°C. Krebs–Henseleit buffer was oxygenated with 95% $O_2$/5% $CO_2$ and maintained at pH 7.4. After 20 min of equilibration, control hearts were perfused for another 20 min while IPC hearts were subjected to four cycles of 5 min of ischaemia and 5 min of reperfusion. Mitochondria were rapidly isolated by differential centrifugation immediately after perfusion or IPC protocols. To prevent SNO breakdown, Langendorff perfusion and sample preparations were carried out in the dark.

## 2.3 Preparation of SSM and IFM from mouse heart

SSM and IFM were isolated following the methods of Palmer *et al.*[24] with minor modifications. As shown in *Figure 1*, immediately following the perfusion or IPC protocol, each heart was quickly weighed and minced in 1 mL of mitochondria isolation buffer (pH7.25, in mmol/L: 225 mannitol, 75 sucrose, 5 MOPS, 2 taurine, 1 EGTA, 1 EDTA, and 0.1 neocuproine). These tissues were then transferred into a small tube and homogenized with a Polytron (Ultra Turrax T25, IKA Labortechnik, set at level 2 with 13 000 rpm) for 3 s. After a 5 min spin at 500 *g* at 4°C, the supernatant was collected for the SSM preparation, while the pellet was subjected to trypsin digestion (5 mg/g pellet) for 10 min on ice. Digestion was stopped by adding isolation buffer containing Halt protease and phosphatase inhibitors (Thermo Scientific, Rockford, IL, USA). Although trypsin digestion was not included in the SSM preparation, a similar amount of protease and phosphatase inhibitors were also added for consistency. Each fraction was centrifuged at 500 *g* for 5 min at 4°C, and the resulting supernatant was spun at 3000 *g* at 4°C for 10 min to pellet SSM and IFM, respectively. Each final sub-population of mitochondria was resuspended in isolation buffer with protease and phosphatase inhibitors. Protein content was determined using a Bradford assay. Since SNO is a very labile thiol-based protein post-translational modification, isolated SSM and IFM were used immediately for SNO and mitochondrial functional analysis without further purification by Percoll gradient ultracentrifugation, which has been reported to alter the redox status of proteins during the sample preparation.[26] Boengler *et al.*[27] have reported that connexin-43 is localized to SSM, we therefore used the presence of connexin-43 as a marker for SSM.

## 2.4 Mitochondrial swelling assay

$Ca^{2+}$-induced swelling of isolated mitochondria was measured spectrophotometrically as a decrease in absorbance at 540 nm using a Fluostar Omega plate reader (BMG Labtech, Ortenberg, Germany). Isolated SSM or IFM (50 μg) were washed twice with mitochondria isolation buffer without EGTA/EDTA and resuspended in swelling buffer (pH 7.4 in mmol/L: 120 KCl, 10 Tris–HCl, 5 MOPS, 5 $Na_2HPO_4$, 10 glutamate, and 2 malate) in the absence and presence of 1 mmol/L of sodium L-ascorbate in a total volume of 100 μL. The mitochondrial swelling was induced by adding 5 μL of 5 mmol/L $CaCl_2$ (0.5 μmol $Ca^{2+}$/mg mitochondrial protein) and the recording of absorbance at 540 nm was continued for 800 s.

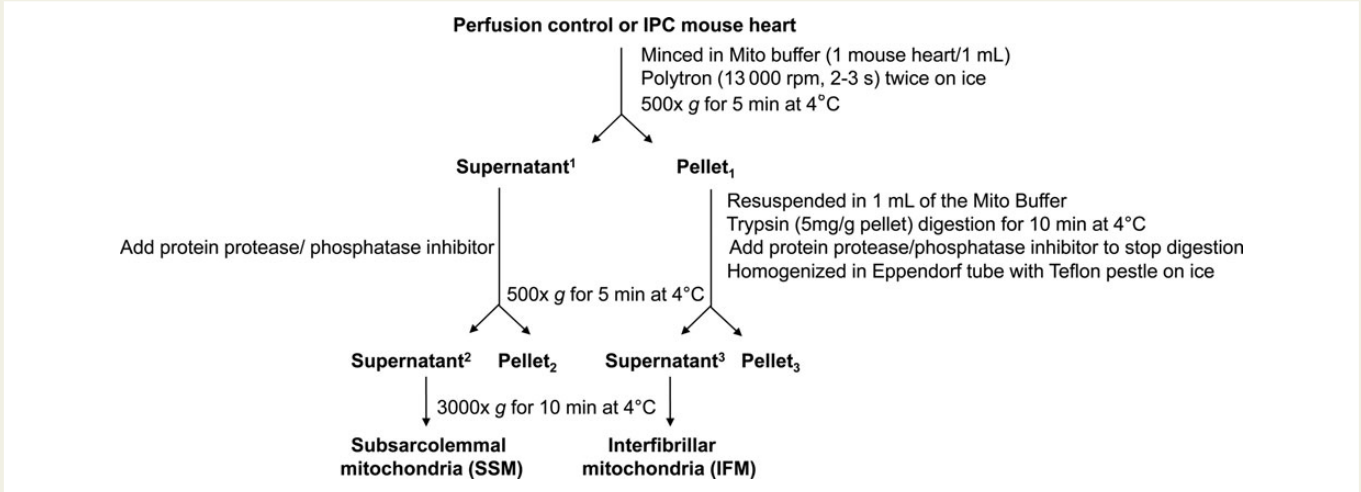


**Figure 1** Protocol for the isolation of SSM and IFM from the perfused mouse heart.

## 2.5 Total SNO content determination and identification of SNO proteins by 2D mono-CyDye-maleimide DIGE

The modified biotin switch method[28] using maleimide sulfhydryl-reactive fluors (Thermo Scientific Pierce Biotechnology, Rockford, IL, USA) was applied to identify SNO proteins.[29,30] After the SNO/dye switch, samples were separated by non-reducing 4–12% Bis–Tris SDS–PAGE in the dark. Total SNO content (DyLight-maleimide 680 intensity) was analysed by scanning each individual sample lane using a Li-Cor Odyssey scanner (Li-Cor Biosciences, Lincoln, NB, USA) at 700 nm. SNO proteins were also analysed by two-dimensional mono-CyDye-maleimide fluorescence difference gel electrophoresis (2D DIGE).[31] Equal amounts (5 μg) of GSNO-treated BSA (BSA-SNO) were subjected to the SNO/dye switch and loaded into the additional sample well on each 2D gel to serve as an internal standard. We compared three samples for each of the four conditions (SSM and IFM under perfusion and IPC) for a total of 12 samples. We ran a total of six gels, with each sample run once. We used the BSA standard to set the fluorescence intensity so we could compare data across the six gels. After 2D DIGE, each gel ($n = 6$) was scanned at the unique excitation/emission wavelength of each dye using a Typhoon 9400 imager (GE Healthcare Life Sciences, Piscataway, NJ, USA) at a resolution of 100 μm. The photomultiplier tube for each wavelength was set to an equal gain intensity based upon the internal BSA-SNO spot. Images from each gel were aligned using the two internal anchor spots and analysed with SameSpots software (TotalLab, Newcastle upon Tyne, UK). The gel was post-stained with Flamingo fluorescent gel stain (Bio-Rad, Hercules, CA, USA) and the protein spots that corresponded to the fluorescent dye pattern were picked. The protein-SNO level of each spot was determined by the ratio of fluorescence intensity for each mono-CyDye-maleimide fluor vs. the fluorescence intensity of the Flamingo protein staining. The Ettan Spot Handling Workstation (GE Healthcare Life Sciences) was used for automated extraction of the selected protein spots followed by in-gel trypsin digestion. After sample extraction from the spot handling workstation, each sample was manually desalted using Millipore C18 Ziptips (EMD Millipore Corporation, Billerica, MA, USA) following the manufacturer's recommendation.

## 2.6 LC–MS/MS analysis and database search

LC–MS/MS was performed using an Eksigent nanoLC-Ultra 1D plus system (Dublin, CA, USA) coupled to an LTQ Orbitrap Elite mass spectrometer (Thermo Fisher Scientific, San Jose, CA, USA) using CID fragmentation. Peptides were first loaded onto an Zorbax 300SB-C18 trap column (Agilent, Palo Alto, CA, USA) at a flow rate of 6 μL/min for 6 min and then separated on a reversed-phase PicoFrit analytical column (New Objective, Woburn, MA, USA) using a short 15-min linear gradient of 5–40% acetonitrile for 2D gel spots. LTQ-Orbitrap Elite settings were as follows: spray voltage 1.5 kV; full MS mass range: $m/z$ 300 to 2000. The LTQ-Orbitrap Elite was operated in a data-dependent mode; i.e. one MS1 high resolution (60 000) scan for precursor ions followed by six data-dependent MS2 scans for precursor ions above a threshold ion count of 500 with collision energy of 35%. The raw file generated from the LTQ Orbitrap Elite was analysed using Proteome Discoverer v1.4 software (Thermo Fisher Scientific, LLC) using our six-processor Mascot cluster at NIH (v.2.4) search engine. The following search criteria was set to: database, Swiss Institute of Bioinformatics (Sprot_544996, 16 676 sequences); taxonomy, mus musculus (mouse); enzyme, trypsin; miscleavages, 2; variable modifications, Oxidation (M), Deamidation (NQ), Acetyl (protein *N*-term), *N*-ethylmaleimide(C); MS peptide tolerance 20 ppm; MS/MS tolerance as 0.8 Da. Protein identifications were accepted based on two or more unique peptides with a false discovery rate (FDR) of 99% or higher and a correct molecular mass identification.

## 2.7 Western blot

After the DyLight switch, equal amounts of total heart homogenate were separated by 4–12% Bis–Tris SDS–PAGE (Life Technologies, Grand Island, NY, USA) under non-reducing conditions. To correct for uneven running of the end lanes, an extra sample and/or blank was randomly loaded onto the two end lanes. After the transfer to a nitrocellulose membrane, the membrane was first scanned for DyLight/SNO signal using a Li-Cor Odyssey scanner, and then stained with Ponceau S. After washing with TBS-T (pH8.0, in mmol/L: 10 Tris, 150 NaCl, and 0.1% (v/v) Tween 20), the membrane was blocked with TBS-T supplemented with 5% (w/v) non-fat dry milk. The antibodies were diluted as follows: 1:10 000 for mouse monoclonal anti-caveolin-3 antibody (#610421, BD Biosciences, San Jose, CA, USA), 1:250 for rabbit polyclonal anti-eNOS antibody (#sc-654, Santa Cruz Biotechnology, Dallas, TX, USA), 1:250 for goat polyclonal anti-VDAC1 antibody (#sc-8828, Santa Cruz), and 1:250 for rabbit polyclonal anti-connexin-43 antibody (#sc-9059, Santa Cruz). The corresponding IgG HRP-conjugated secondary antibodies (1:5,000 dilution, Cell Signaling, Danvers, MA, USA) were used in combination with a chemiluminescent substrate (GE Healthcare Life Sciences) according to standard procedures.

## 2.8 Data analysis

Results are expressed as mean ± SE. Statistical significance was determined by two-way ANOVA with alpha-level set at 0.05 followed by a *post-hoc* Bonferroni test among multiple groups, or by an unpaired two-tailed Student's *t*-test between two groups.

# 3. Results

We previously reported that IPC leads to an increase in SNO of mitochondrial proteins.[29,32] Interestingly, two populations of mitochondria (i.e. SSM and IFM) are distributed in cardiomyocytes. Given the close proximity of SSM to caveolae at the sarcolemma, and the compact compartmentalization of IFM among the contractile myofibrils, we tested the hypothesis that caveolae-mediated cardioprotective signalling preferentially target SSM rather than IFM.

## 3.1 IPC increased SNO content preferentially in SSM

Following control perfusion or IPC treatment in Langendorff perfused mouse hearts, SSM and IFM were immediately isolated. To prevent the decomposition of SNO, EDTA (1 mM) and neocuproine (0.1 mM, a specific copper chelator) were added to the mitochondrial isolation buffer and the isolation procedure was performed in the dark. Since SNO is a very labile thiol-based protein post-translational modification, isolated SSM and IFM were used immediately for SNO/DyLight switch. After the DyLight switch using DyLight 680-maleimide, both SSM and IFM isolated from perfusion control and IPC WT hearts were subjected to a 1D non-reducing 4–12% Bis–Tris SDS–PAGE in the dark. The total DyLight 680 fluorescence intensity/SNO content in each sample was determined by gel scanning using a Li-Cor Odyssey scanner at the 700 nm channel. As shown in *Figure 2*, in perfusion control hearts, SSM had a higher SNO content than IFM. Interestingly, IPC only led to increased SNO in SSM but not in IFM, suggesting that SSM may be preferentially targeted by caveolae-derived eNOS/NO/SNO signalling.

## 3.2 Increased SNO proteins in SSM identified by 2D mono-CyDye-maleimide DIGE

The 2D mono-CyDye-maleimide DIGE proteomic technique was applied to verify whether IPC-induced caveolae-associated eNOS/NO/SNO signalling preferentially targets to SSM. Compared with DyLight-maleimide fluorescent dye which carries 3–4 negative charges, the mono-CyDye-maleimide dye is neutral, and therefore it

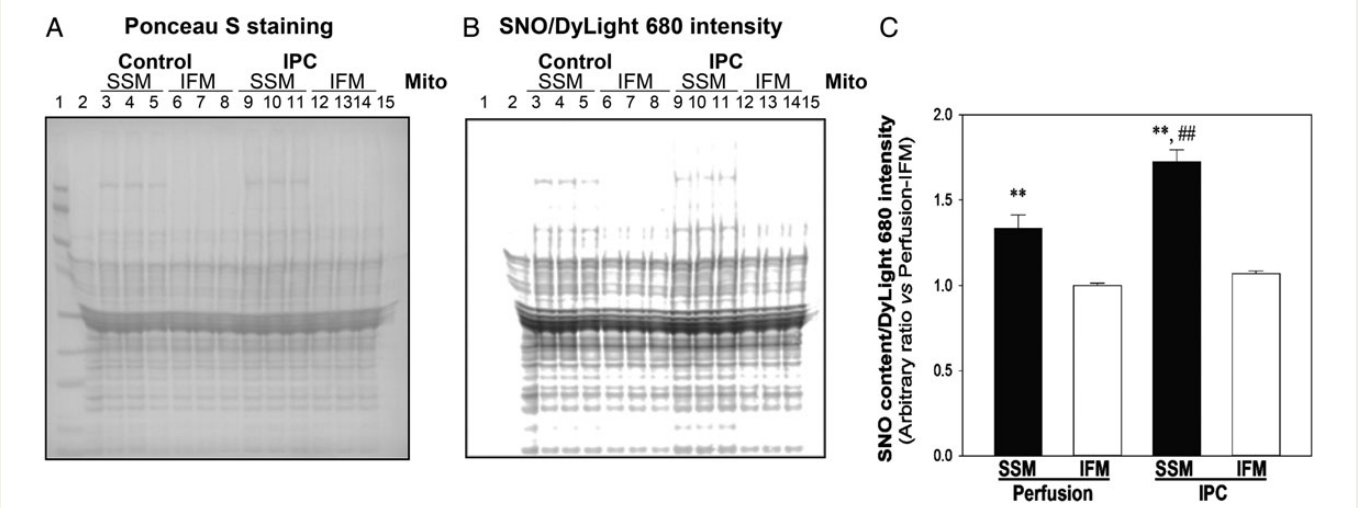


**Figure 2** IPC preferentially increased protein SNO in SSM in mouse hearts. (*A*) Representative Ponceau S staining of membrane after DyLight switch and non-reducing SDS–PAGE. Lanes 2 and 15 were loaded with a perfusion-IFM and blank, respectively. (*B*) The corresponding SNO content/DyLight 680 intensity Li-Cor scanned image. (*C*) The statistical analysis for total SNO content/DyLight 680 intensity from each sample, $^{**}P < 0.01$ vs. Perfusion-IFM; $^{\#\#}P < 0.01$ vs. Perfusion-SSM ($n = 6$ per group).

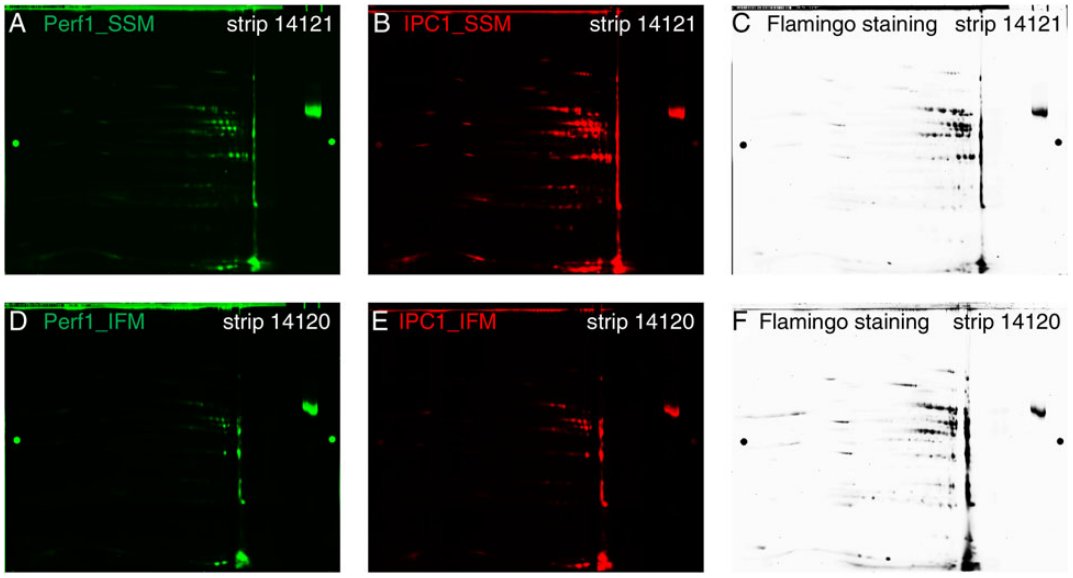


**Figure 3** 2D mono-CyDye-maleimide DIGE for protein SNO analysis. Equal amounts of protein from individual mitochondrial preparations were labelled with individual mono-CyDye-maleimide. Equal amounts (5 μg) of GSNO-treated BSA (BSA-SNO) were subjected to the SNO/dye switch and loaded into the additional sample well on each 2D gel to serve as an internal standard. After 2D DIGE, gels from three independent experiments were scanned at the distinct wavelengths for each fluor, showing a pattern of protein SNO for each treatment group. Representative SNO/mono-CyDye-maleimide images: Perf1-SSM (*A*) vs. IPC1-SSM (*B*) in 2D gel for IEF strip 14121, and Perf1-IFM (*D*) vs. IPC1-IFM (*E*) in 2D gel for IEF strip 14 120. The gel was post-stained with Flamingo fluorescent gel stain, as shown for each corresponding 2D gel (*C* and *F*).

does not lead to a significant shift in the pI of the spot. Thus, the labelled SNO-modified proteins overlay well with the Flamingo-stained proteins. Since there are only two mono-CyDye-maleimide dyes available, only two samples can be individually labelled and subjected to a 2D DIGE gel analysis. A total of six 2D DIGE gels were processed for SSM/IFM samples isolated from control and IPC hearts ($n = 3$ in each group). Equal amounts (5 μg) of GSNO-treated BSA (BSA-SNO) were subjected to the SNO/dye switch and loaded into the additional sample well on each 2D gel to serve as an internal standard. In addition, the protein-SNO level of each spot was determined by the ratio of mono-CyDye-maleimide fluorescent intensity vs. Flamingo-stained protein fluorescent intensity.

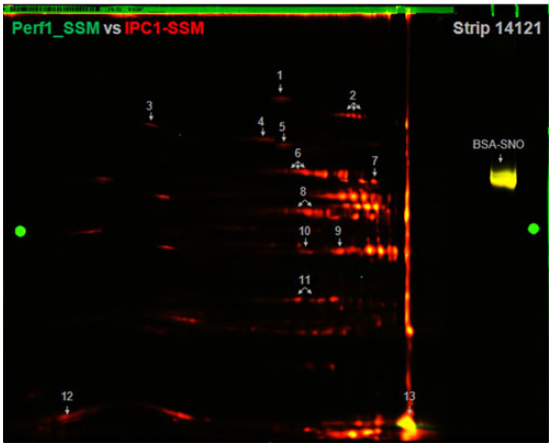


**Figure 4** IPC increased protein-SNO in SSM as determined via 2D mono-CyDye-maleimide DIGE. Representative overlaid images of Perf1-SSM and IPC1-SSM from one 2D mono-CyDye-maleimide DIGE gel. Protein spots with a number labelled on top showing a change of at least 50% or higher in IPC-SSM compared with Perf-SSM were picked for MS/MS analysis, the identifications are listed in *Table 1*.

The representative images of 2D mono-CyDye-maleimide DIGE and Flamingo protein staining from one set of experiments are shown in *Figure 3*. The fluorescent overlay image (*Figure 4*) shows a significant increase in protein SNO in SSM in IPC-treated hearts compared with perfusion control. Data from three independent experiments are compiled in *Table 1*. Consistent with the results from the 1D SDS–PAGE (*Figure 2*), protein SNO was higher in SSM than IFM in perfusion control hearts. Furthermore, IPC results in an increase in SNO in SSM compared with IFM, and IPC leads to a significant increase in SNO proteins in SSM compared with perfusion-SSM. These data support the hypothesis that IPC results in the mobilization and translocation of caveolae-associated eNOS/NO/SNO signalling preferentially to SSM.

## 3.3 IPC led to the increased association of eNOS with SSM

Numerous studies have demonstrated that eNOS is localized in caveolae via interaction with caveolin, and this compartmentalization facilitates dynamic protein–protein interactions and signal transduction events that modify eNOS activity.[14,33,34] Caveolin-3 has been shown to be the muscle-specific caveolin.[35,36] Anti-eNOS and anti-caveolin-3 immunoblots were employed to study the distribution of these signalling molecules in these two mitochondrial sub-populations isolated from

**Table 1 IPC-induced increase in protein SNO in SSM identified by 2D mono-CyDye-maleimide DIGE**

| Spot | Protein name | Accession number | Mw (kDa) | Protein pI | SNO CyDye fluorescent intensity vs. Flamingo protein staining intensity | | | |
|---|---|---|---|---|---|---|---|---|
| | | | | | Perf-SSM | Perf-IFM | IPC-SSM | IPC-IFM |
| 1 | 2-oxoglutarate dehydrogenase | Q60597 | 116.4 | 6.83 | $1.54 \pm 0.12^{a}$ | $0.34 \pm 0.05$ | $2.40 \pm 0.08^{b,c}$ | $0.47 \pm 0.12^{d}$ |
| 2 | Aconitate hydratase | Q99KI0 | 85.4 | 7.93 | $0.94 \pm 0.15^{a}$ | $0.44 \pm 0.05$ | $2.53 \pm 0.22^{b,c}$ | $0.62 \pm 0.16^{d}$ |
| | | | | | $0.39 \pm 0.08^{a}$ | $0.15 \pm 0.03$ | $1.22 \pm 0.18^{b,c}$ | $0.26 \pm 0.08^{d}$ |
| | | | | | $1.07 \pm 0.05^{a}$ | $0.35 \pm 0.12$ | $2.90 \pm 0.01^{b,c}$ | $0.37 \pm 0.08$ |
| 3 | Stress-70 protein | P38647 | 73.4 | 6.07 | $0.55 \pm 0.10^{a}$ | $0.25 \pm 0.03$ | $1.72 \pm 0.23^{b,c}$ | $0.36 \pm 0.08^{d}$ |
| 4 | Succinate dehydrogenase flavoprotein subunit | Q8K2B3 | 72.5 | 7.37 | $1.06 \pm 0.11^{a}$ | $0.34 \pm 0.09$ | $2.59 \pm 0.23^{b,c}$ | $0.53 \pm 0.15^{d}$ |
| 5 | Electron transfer flavoprotein dehydrogenase | Q921G7 | 68.0 | 7.58 | $0.38 \pm 0.12^{a}$ | $0.19 \pm 0.04$ | $1.69 \pm 0.10^{b,c}$ | $0.36 \pm 0.10^{d}$ |
| 6 | F1-ATPase subunit α | Q03265 | 59.7 | 9.19 | $0.53 \pm 0.09^{a}$ | $0.21 \pm 0.01$ | $1.80 \pm 0.28^{b,c}$ | $0.35 \pm 0.06^{d}$ |
| | | | | | $0.21 \pm 0.07^{a}$ | $0.11 \pm 0.04$ | $1.33 \pm 0.24^{b,c}$ | $0.34 \pm 0.16^{d}$ |
| | | | | | $0.28 \pm 0.03^{a}$ | $0.17 \pm 0.08$ | $0.67 \pm 0.06^{b,c}$ | $0.16 \pm 0.03$ |
| 7 | Fumarate hydratase | P97807 | 54.3 | 9.04 | $1.40 \pm 0.06^{a}$ | $0.70 \pm 0.05$ | $3.18 \pm 0.27^{b,c}$ | $0.72 \pm 0.14$ |
| 8 | Long-chain specific acyl-CoA dehydrogenase | P51174 | 47.9 | 8.31 | $0.47 \pm 0.06^{a}$ | $0.24 \pm 0.03$ | $1.48 \pm 0.26^{b,c}$ | $0.45 \pm 0.12^{d}$ |
| | | | | | $0.68 \pm 0.03^{a}$ | $0.50 \pm 0.05$ | $1.72 \pm 0.27^{b,c}$ | $0.57 \pm 0.14$ |
| 9 | Malate dehydrogenase | P08249 | 35.6 | 8.68 | $0.90 \pm 0.11^{a}$ | $0.40 \pm 0.04$ | $2.31 \pm 0.11^{b,c}$ | $0.68 \pm 0.13^{d}$ |
| 10 | Electron transfer flavoprotein subunit α | Q99LC5 | 35.0 | 8.38 | $0.77 \pm 0.01^{a}$ | $0.59 \pm 0.12$ | $2.16 \pm 0.12^{b,c}$ | $0.87 \pm 0.08^{d}$ |
| 11 | Electron transfer flavoprotein subunit β | Q9DCW4 | 27.6 | 8.10 | $0.49 \pm 0.03^{a}$ | $0.22 \pm 0.02$ | $1.22 \pm 0.03^{b,c}$ | $0.42 \pm 0.12^{d}$ |
| | | | | | $0.73 \pm 0.09$ | $0.63 \pm 0.14$ | $2.47 \pm 0.13^{b,c}$ | $0.51 \pm 0.02$ |
| 12 | Cytochrome *c* oxidase subunit 5A | P12787 | 16.1 | 6.54 | $1.63 \pm 0.03^{a}$ | $0.72 \pm 0.08$ | $3.99 \pm 0.49^{b,c}$ | $0.54 \pm 0.06$ |
| 13 | Cytochrome *c* | P62897 | 11.6 | 9.58 | $1.39 \pm 0.11^{a}$ | $0.94 \pm 0.04$ | $2.79 \pm 0.06^{b,c}$ | $0.97 \pm 0.06$ |

Protein identifications with a false discovery rate (FDR) of 99% or higher were accepted based on the highest score with two or more unique peptides, and a correct molecular mass identification. $n = 3$ in each group.
[a]$P < 0.05$ vs. Perf-IFM.
[b]$P < 0.05$ vs. IPC-IFM.
[c]$P < 0.05$ vs. Perf-SSM.
[d]$P < 0.05$ vs. Perf-IFM.

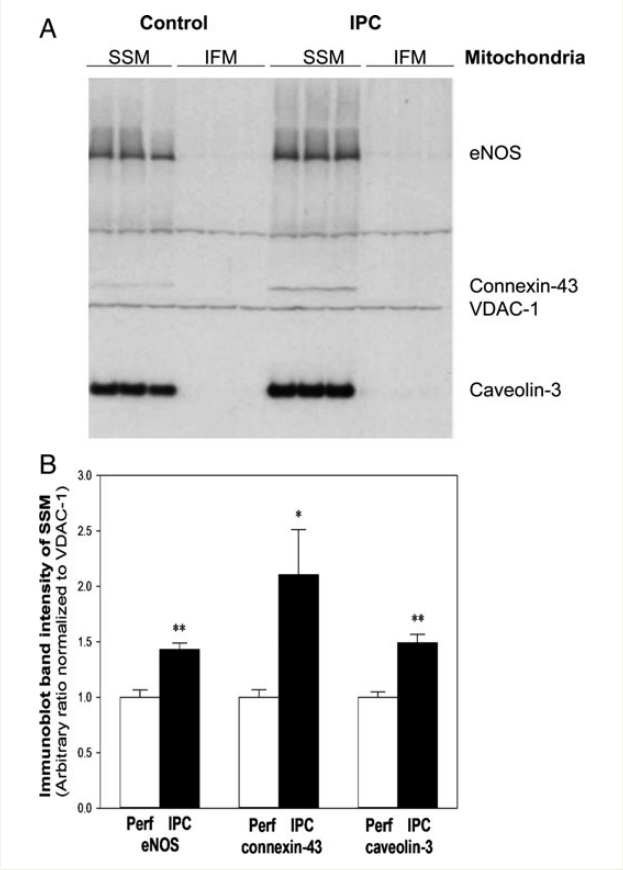


**Figure 5** IPC led to an increased association of eNOS with SSM in mouse hearts. (*A*) Representative anti-eNOS, anti-connexin-43, anti-VDAC1, and anti-caveolin-3 western blots; (*B*) Combined analysis ($n = 6$) for immunoblotting band densitometry normalized to VDAC-1 in each SSM group. *$P < 0.05$; **$P < 0.01$ vs. Perfusion-SSM in each group.

mouse hearts. As shown in *Figure 5*, eNOS and caveolin-3 are only found to be associated with SSM, but not with IFM, and the levels of these proteins associated with SSM are increased in mouse hearts following IPC. These results agree with the findings of Boengler *et al.*[27] showing that connexin-43 is localized to SSM and the distribution of connexin-43 in cardiomyocyte SSM is increased with IPC, thereby suggesting a preferential cardioprotective signalling mechanism to SSM.[37] In this study, we only detected connexin-43 in SSM but not in IFM isolated from mouse hearts. In addition, IPC lead to an increase in the translocation of connexin-43 to SSM (*Figure 5*).

## 3.4 IPC did not cause an increase in SNO and did not enhance the association of eNOS to SSM in caveolin-3$^{-/-}$ hearts

It has been shown that the disruption of caveolae, either by cholesterol sequestering agent treatment[7,8] or genetic deletion of the protein caveolin-3,[7] leads to the loss of IPC-induced cardioprotection. In this study, we further tested whether there is disrupted caveolin-3/eNOS/SNO signalling in caveolin-3$^{-/-}$ mouse hearts subjected to IPC. In contrast to WT hearts (*Figure 6*), IPC did not lead to an increase in SNO in SSM isolated from caveolin-3$^{-/-}$ mouse hearts. Similar to WT hearts, eNOS was only detected in SSM but not in IFM from caveolin-3$^{-/-}$ mouse hearts. However, IPC did not increase the association of eNOS with SSM (*Figure 7*).

## 3.5 Effect of *S*-nitrosylation on mitochondrial function

Our previous studies have shown that IPC led to an increase of SNO,[8,29,38] and the protective effect of IPC could be abolished by ascorbate treatment.[8] Ascorbate is a reducing agent that decomposes SNO.[28] The effect of the IPC-induced increase of mitochondrial SNO on mitochondrial function was studied using the $Ca^{2+}$-induced mitochondrial swelling assay. As shown in *Figure 8*, SSM or IFM isolated from IPC hearts both showed less $Ca^{2+}$-induced mitochondrial swelling

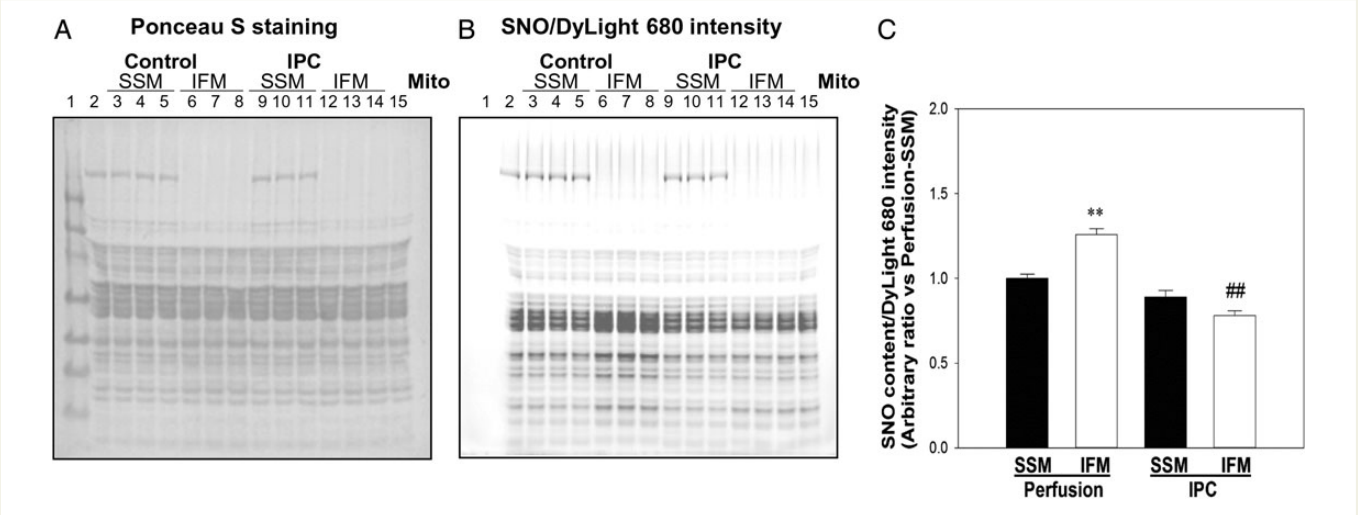


**Figure 6** IPC did not increase protein SNO in SSM in caveolin-3$^{-/-}$ hearts. (*A*) Representative Ponceau S staining of membrane after DyLight switch and non-reducing SDS–PAGE. Lanes 2 and 15 were loaded with a Perfusion-SSM and IPC-IFM, respectively. (*B*) The corresponding SNO content/DyLight 680 intensity Li-Cor scanned image. (*C*) The statistical analysis for total SNO content/DyLight 680 intensity from each sample, **$P < 0.01$ vs. Perfusion-SSM; $^{\#\#}P < 0.01$ vs. Perfusion-IFM ($n = 3$ per group).

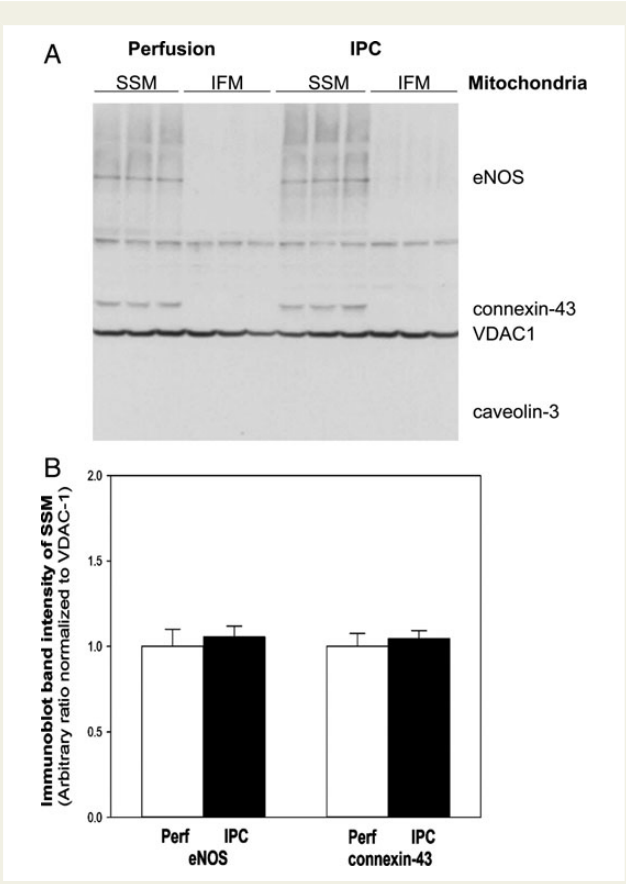


**Figure 7** IPC did not increase association of eNOS to SSM in caveolin-3$^{-/-}$ hearts. (*A*) Representative anti-eNOS, anti-connexin-43, anti-VDAC1, and anti-caveolin-3 western blots; (*B*) Combined analysis ($n = 6$) for immunoblotting band densitometry normalized to VDAC-1 in each SSM group.

compared with corresponding perfusion control group. However, the protection observed in the SSM was dependent upon SNO, as the protection observed in the SSM was significantly attenuated by ascorbate treatment.

# 4. Discussion

Structural and functional differences between SSM and IFM have been observed in cardiac mitochondria.[24,25] High-resolution scanning electron microscopy analysis showed ultrastructural differences between the two sub-populations in rat cardiomyocytes, with SSM having more lamelliform and less tubular cristae than IFM.[25] Furthermore, there are data to suggest that SSM might be more susceptible to I/R damage compared with IFM,[39,40] not only because SSM apparently have less resistance to I/R-induced mitochondrial permeability transition (MPT) than IFM, but also this sub-population of mitochondria would have a higher oxygen gradient exposure during I/R compared with IFM. Although ischaemic myocardium can be salvaged via myocardial reperfusion, irreversible injury also occurs during reperfusion. Given that SSM are $<10\%$ of the total mitochondria, one might question why they have a disproportional influence on cell death. The most likely cause of myocyte death during I/R injury is the disruption of cellular membranes and the loss of sarcolemmal integrity.[41] Since the SSM have been reported to play an important role in regulation of ionic homeostasis and thus plasma membrane integrity,[42,43] the damage to these mitochondria (even though only 10%) could set off a cascade leading to disruption of sarcolemmal integrity and cell death. Therefore, the modulation of this population of mitochondria could be crucial for cardioprotection. It has been proposed by Chen *et al.*[40] that the targets of PostC-induced cytoprotective signalling are mitochondria damaged by ischaemia, and that the benefits of PostC on mitochondrial function were observed in SSM but not in IFM. Also, despite enhanced susceptibility to stress, SSM were more responsive to the protective effect of diazoxide compared with IFM.[44]

Mitochondria are thought to be a central player or end effector in cell death, and many cardioprotective signalling mechanisms have been found to converge on the mitochondria and reduce cell death.[1,2] NO-mediated SNO signalling has been shown to play an important role in IPC-induced cardioprotection,[22,23,29] and mitochondrial proteins are major SNO targets.[29,32,45] In this study, we provided additional evidence that IPC-induced increase of eNOS/NO/SNO signalling preferentially regulates SSM. Interestingly, neither caveolin-3 nor eNOS was detected in IFM preparations, suggesting that caveolae-associated signalling might have a preferential impact on the (sub)sarcolemmal subcellular microenvironment.

Other groups have suggested that activated eNOS can be internalized to deliver NO to subcellular targets for biological effects.[46–48] We have previously shown that MβCD (a cholesterol sequestering agent) treatment not only disrupted caveolae and the association of eNOS with caveolin-3, but also blocked IPC-induced cardioprotection and the increase of mitochondrial SNO proteins.[8] These data are consistent with the hypothesis that caveolin-3-associated eNOS/NO trafficking between plasma membrane and mitochondria provide an important signalling pathway regulating SNO of mitochondrial proteins. In this study, the findings of an IPC-induced increase of caveolae-associated eNOS/NO/SNO signalling to SSM are consistent with this hypothesis. The data in this paper (*Table 1*) show a typical 2-fold increase of SNO in SSM compared with IFM. Furthermore, after IPC, the SNO difference between SSM and IFM is enhanced such that there is roughly a 4-fold increase SNO in SSM vs. IFM after IPC. This preferential SNO signalling to SSM could enhance protection to SSM, which have been reported to have increased susceptibility to I/R damage.[40,49]

All of proteins that showed an IPC-induced increase in SNO (*Table 1*) have been also reported in our previous studies.[8,29,32] Of the 19 spots arising from 13 proteins (see *Table 1*), seven spots showed a significant increase in SNO in SSM, but not in IFM. We speculate that SNO of these seven proteins could play a role in cardioprotection. These seven proteins include, aconitase, F1-ATP synthase subunit α, fumarate hydratase, long-chain specific acyl-CoA dehydrogenase, electron transfer flavoprotein β, cytochrome *c* oxidase subunit 5A, and cytochrome *c*. F1-ATP synthase subunit α is a promising candidate as we have shown that IPC led to an increase in SNO of the mitochondrial F1-ATPase subunit α with a concomitant decrease in its activity.[29] The inhibition of the F1-ATPase by *S*-nitrosylation during ischaemia could be beneficial by conserving cytosolic ATP, since during ischaemia as much as 50% of the glycolytically generated ATP is consumed by reverse mode of the F1-ATPase.[29] Furthermore, Wang *et al.*[50] have demonstrated oxidation of C294 in the α subunit (associated with disulfide bond between the α and γ subunits) of F1-ATPase which is associated with inhibition of F1-ATPase activity in dyssynchronous heart failure. Interestingly, they further show that cardiac resynchronization therapy leads to *S*-nitrosylation of C294 of the α subunit along with recovery of the ATP synthase activity.

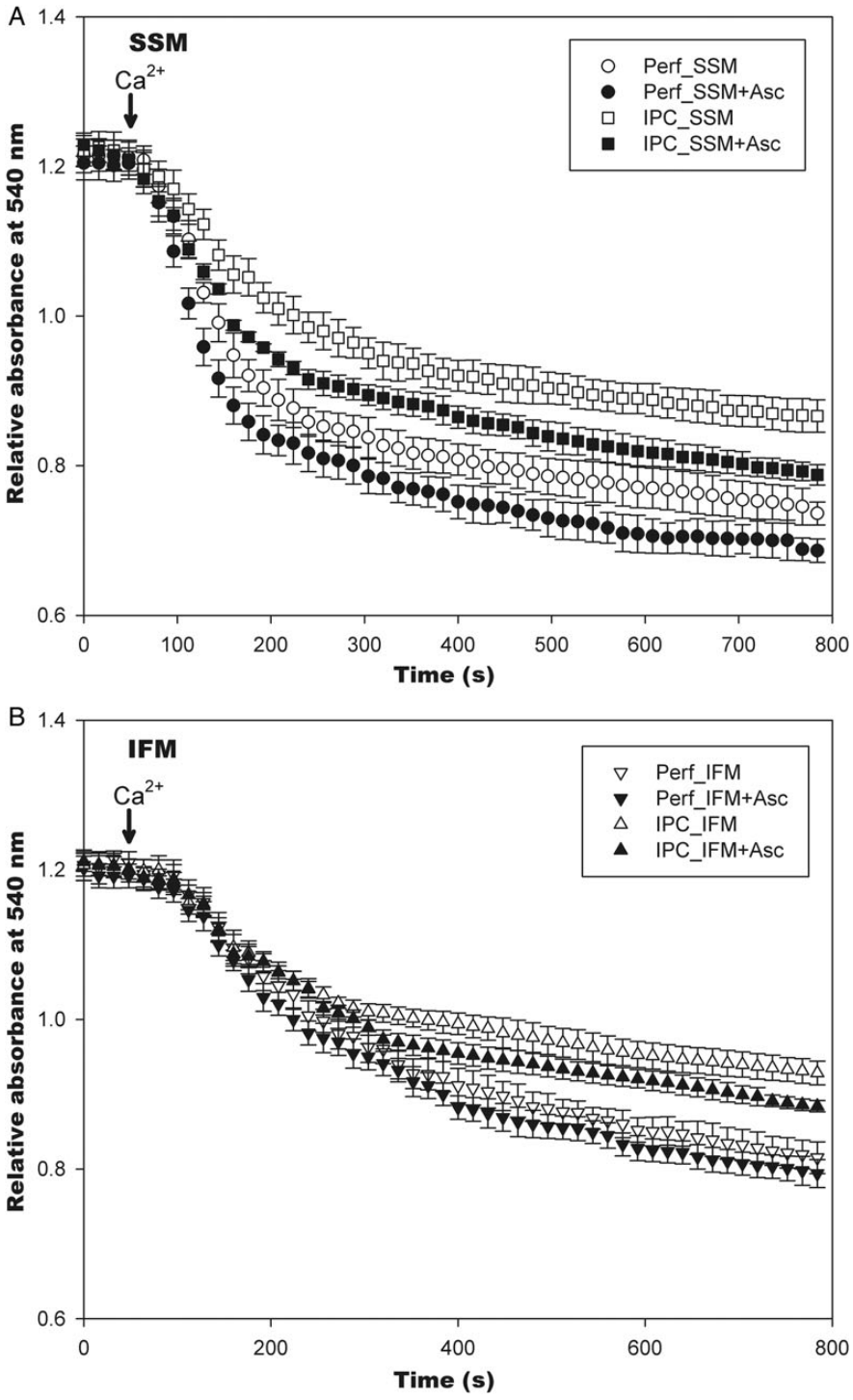


**Figure 8** Decomposition of SNO by ascorbate treatment exacerbated $Ca^{2+}$-induced mitochondrial swelling. Intact mitochondria, SSM (*A*), and IFM (*B*), isolated from perfusion control and IPC mouse hearts ($n = 3$ per group) were pre-treated with or without sodium L-ascorbate (1 mmol/L). The mitochondrial swelling was induced by adding $Ca^{2+}$ (0.5 μmol $Ca^{2+}$/mg mitochondrial protein) and monitored at 540 nm spectrophotometrically using Fluostar Omega plate reader (BMG Labtech). The results represent average measurements from three independent preparations isolated from a pair of mouse hearts subjected to perfusion control and IPC, respectively.

An altered conformation of the F1-ATPase has been proposed to predispose mitochondria to undergo MPT which has been suggested to be the mediator of necrotic cell death. It is tempting to speculate that perhaps SNO of the α subunit of the F1-ATPase, by inhibiting crosslinking between the α and γ subunits, might contribute to the decreased susceptibility to MPT.

There are some limitations that should be considered. Since SNO signalling is a very labile post-translational protein modification, we did not

purify the mitochondria using Percoll gradient ultracentrifugation, as it has been reported that mitochondrial proteins are susceptible to excessive oxidation during preparation.[26] Therefore, we cannot rule out the possibility that the increased association of eNOS and caveolin-3 is due to increased sarcolemmal contamination in SSM during sample preparation. However, it is not clear why this contamination would increase with IPC. Furthermore, the differences observed in SNO levels of mitochondrial proteins between SSM and IFM cannot easily be explained by plasma membrane contamination.

In summary, this study is the first to demonstrate that SSM are major targets for protein SNO in IPC mouse hearts, suggesting that SSM may be preferentially targeted and regulated by caveolae/sarcolemma-derived signalling and post-translational protein modification (i.e. caveolae-derived eNOS/NO/SNO). This provides evidence in support of the hypothesis that the two sub-populations of mitochondria in the myocardium may respond differently to stress and cardioprotective signalling, and thus play different roles in health and disease.

**Conflict of interest:** none declared.

## Funding

This work was supported by the NIH Intramural Program (J.S., T.N., A.A., S.M., and E.M.), 1K99HL114721 (M.K.), 5R01HL039752 (C.S.), HL091071 (H.H.P.), HL107200 (H.H.P. and D.M.R.), HL066941 (D.M.R. and H.H.P.), VA Merit BX001963 (H.H.P.), and VA Merit BX000783 (D.M.R.).

## References

1. Murphy E, Steenbergen C. Preconditioning: the mitochondrial connection. *Annu Rev Physiol* 2007;**69**:51–67.
2. Penna C, Perrelli MG, Pagliaro P. Mitochondrial pathways, permeability transition pore, and redox signaling in cardioprotection: therapeutic implications. *Antioxid Redox Signal* 2012;**18**:556–599.
3. Garlid KD, Costa AD, Quinlan CL, Pierre SV, Dos Santos P. Cardioprotective signaling to mitochondria. *J Mol Cell Cardiol* 2009;**46**:858–866.
4. Quinlan CL, Costa ADT, Costa CL, Pierre SV, Dos Santos P, Garlid KD. Conditioning the heart induces formation of signalosomes that interact with mitochondria to open mito-KATP channels. *Am J Physiol* 2008;**295**:H953–H961.
5. Wang J, Schilling JM, Niesman IR, Headrick JP, Finley JC, Kwan E, Patel PM, Head BP, Roth DM, Yue Y, Patel HH. Cardioprotective trafficking of caveolin to mitochondria is Gi-protein dependent. *Anesthesiology* 2014;**121**:538–548.
6. Wong R, Aponte AM, Steenbergen C, Murphy E. Cardioprotection leads to novel changes in the mitochondrial proteome. *Am J Physiol* 2010;**298**:H75–H91.
7. Horikawa YT, Patel HH, Tsutsumi YM, Jennings MM, Kidd MW, Hagiwara Y, Ishikawa Y, Insel PA, Roth DM. Caveolin-3 expression and caveolae are required for isoflurane-induced cardiac protection from hypoxia and ischemia/reperfusion injury. *J Mol Cell Cardiol* 2008;**44**:123–130.
8. Sun J, Kohr MJ, Nguyen T, Aponte AM, Connelly PS, Esfahani SG, Gucek M, Daniels MP, Steenbergen C, Murphy E. Disruption of caveolae blocks ischemic preconditioning-mediated S-nitrosylation of mitochondrial proteins. *Antioxid Redox Signal* 2012;**16**:45–56.
9. Tsutsumi YM, Horikawa YT, Jennings MM, Kidd MW, Niesman IR, Yokoyama U, Head BP, Hagiwara Y, Ishikawa Y, Miyanohar A, Patel PM, Insel PA, Patel HH, Roth DM. Cardiac-specific overexpression of caveolin-3 induces endogenous cardiac protection by mimicking ischemic preconditioning. *Circulation* 2008;**118**:1979–1988.
10. Fridolfsson HN, Kawaraguchi Y, Ali SS, Panneerselvam M, Niesman IR, Finley JC, Kellerhals SE, Migita MY, Okada H, Moreno AL, Jennings M, Kidd MW, Bonds JA, Balijepalli RC, Ross RS, Patel PM, Miyanohara A, Chen Q, Lesnefsky EJ, Head BP, Roth DM, Insel PA, Patel HH. Mitochondria-localized caveolin in adaptation to cellular stress and injury. *FASEB J* 2012;**26**:4637–4649.
11. Insel PA, Head BP, Ostrom RS, Patel HH, Swaney JS, Tang CM, Roth DM. Caveolae and lipid rafts: G protein-coupled receptor signaling microdomains in cardiac myocytes. *Ann N Y Acad Sci* 2005;**1047**:166–172.
12. Patel HH, Murray F, Insel PA. Caveolae as organizers of pharmacologically relevant signal transduction molecules. *Annu Rev Pharmacol Toxicol* 2008;**48**:359–391.
13. Feron O, Balligand J-L. Caveolins and the regulation of endothelial nitric oxide synthase in the heart. *Cardiovasc Res* 2006;**69**:788–797.
14. Michel T, Vanhoutte P. Cellular signaling and NO production. *Pflügers Arch* 2010;**459**:807–816.
15. Post H, Schulz R, Behrends M, Gres P, Umschlag C, Heusch G. No involvement of endogenous nitric oxide in classical ischemic preconditioning in swine. *J Mol Cell Cardiol* 2000;**32**:725–733.
16. Nakano A, Liu GS, Heusch G, Downey JM, Cohen MV. Exogenous nitric oxide can trigger a preconditioned state through a free radical mechanism, but endogenous nitric oxide is not a trigger of classical ischemic preconditioning. *J Mol Cell Cardiol* 2000;**32**:1159–1167.
17. Guo Y, Li Q, Wu W-J, Tan W, Zhu X, Mu J, Bolli R. Endothelial nitric oxide synthase is not necessary for the early phase of ischemic preconditioning in the mouse. *J Mol Cell Cardiol* 2008;**44**:496–501.
18. Talukder MAH, Yang F, Shimokawa H, Zweier JL. eNOS is required for acute in vivo ischemic preconditioning of the heart: effects of ischemic duration and sex. *Am J Physiol* 2010;**299**:H437–H445.
19. Andreadou I, Iliodromitis EK, Rassaf T, Schulz R, Papapetropoulos A, Ferdinandy P. The role of gasotransmitters NO, $H_2S$ and CO in myocardial ischaemia/reperfusion injury and cardioprotection by preconditioning, postconditioning and remote conditioning. *Br J Pharmacol* 2014; doi: 10.1111/bph.12811.
20. Lima B, Forrester MT, Hess DT, Stamler JS. S-Nitrosylation in cardiovascular signaling. *Circ Res* 2010;**106**:633–646.
21. Schulman IH, Hare JM. Regulation of cardiovascular cellular processes by S-nitrosylation. *Biochim Biophys Acta* 2012;**1820**:752–762.
22. Sun J, Murphy E. Protein S-nitrosylation and cardioprotection. *Circ Res* 2010;**106**:285–296.
23. Sun J. Protein S-nitrosylation: a role of nitric oxide signaling in cardiac ischemic preconditioning. *Acta Physiol Sin* 2007;**59**:544–552.
24. Palmer JW, Tandler B, Hoppel CL. Biochemical properties of subsarcolemmal and interfibrillar mitochondria isolated from rat cardiac muscle. *J Biol Chem* 1977;**252**:8731–8739.
25. Riva A, Tandler B, Loffredo F, Vazquez E, Hoppel C. Structural differences in two biochemically defined populations of cardiac mitochondria. *Am J Physiol* 2005;**289**:H868–H872.
26. Chang AHK, Sancheti H, Garcia J, Kaplowitz N, Cadenas E, Han D. Respiratory substrates regulate S-nitrosylation of mitochondrial proteins through a thiol-dependent pathway. *Chem Res Toxicol* 2014;**27**:794–804.
27. Boengler K, Stahlhofen S, van de Sand A, Gres P, Ruiz-Meana M, Garcia-Dorado D, Heusch G, Schulz R. Presence of connexin 43 in subsarcolemmal, but not in interfibrillar cardiomyocyte mitochondria. *Basic Res Cardiol* 2009;**104**:141–147.
28. Jaffrey SR, Snyder SH. The biotin switch method for the detection of S-nitrosylated proteins. *Sci STKE* 2001;**86**:PL1.
29. Sun J, Morgan M, Shen R-F, Steenbergen C, Murphy E. Preconditioning results in S-nitrosylation of proteins involved in regulation of mitochondrial energetics and calcium transport. *Circ Res* 2007;**101**:1155–1163.
30. Lin J, Steenbergen C, Murphy E, Sun J. Estrogen receptor-β activation results in S-nitrosylation of proteins involved in cardioprotection. *Circulation* 2009;**120**:245–254.
31. Tong G, Aponte AM, Kohr MJ, Steenbergen C, Murphy E, Sun J. Postconditioning leads to an increase in protein S-nitrosylation. *Am J Physiol* 2014;**306**:H825–H832.
32. Kohr MJ, Sun J, Aponte A, Wang G, Gucek M, Murphy E, Steenbergen C. Simultaneous measurement of protein oxidation and S-nitrosylation during preconditioning and ischemia/reperfusion injury with resin-assisted capture. *Circ Res* 2011;**108**:418–426.
33. Shaul PW. Regulation of endothelial nitric oxide synthase: location, location, location. *Annu Rev Physiol* 2002;**64**:749–774.
34. Dessy C, Feron O, Balligand J-L. The regulation of endothelial nitric oxide synthase by caveolin: a paradigm validated in vivo and shared by the 'endothelium-derived hyperpolarizing factor'. *Pflügers Arch* 2010;**459**:817–827.
35. Feron O, Belhhassen L, Kobzik L, Smith TW, Kelly RA, Michel T. Endothelial nitric oxide synthase targeting to caveolae. Specific interactions with caveolin isoforms in cardiac myocytes and endothelial cells. *J Biol Chem* 1996;**271**:22810–22814.
36. Song KS, Scherer PE, Tang Z, Okamoto T, Li S, Chafel M, Chu C, Kphtz DS, Lisanti MP. Expression of caveolin-3 in skeletal, cardiac, and smooth muscle cells. Caveolin-3 is a component of the sarcolemma and co-fractionates with dystrophin and dystrophin-associated glycoproteins. *J Biol Chem* 1996;**271**:15160–15165.
37. Boengler K, Dodoni G, Rodriguez-Sinovas A, Cabestrero A, Ruiz-Meana M, Gres P, Konietzka I, Lopez-Iglesias C, Carcia-Dorado D, Di Lisa F, Heusch G, Schulz R. Connexin 43 in cardiomyocyte mitochondria and its increase by ischemic preconditioning. *Cardiovasc Res* 2005;**67**:234–244.
38. Sun J, Aponte AM, Kohr MJ, Tong G, Steenbergen C, Murphy E. Essential role of nitric oxide in acute ischemic preconditioning: S-Nitros(yl)ation versus sGC/cGMP/PKG signaling? *Free Radic Biol Med* 2013;**54**:105–112.
39. Palmer JW, Tandler B, Hoppel CL. Heterogeneous response of subsarcolemmal heart mitochondria to calcium. *Am J Physiol* 1986;**250**:H741–H748.
40. Chen Q, Paillard M, Gomez L, Li H, Hu Y, Lesnefsky EJ. Postconditioning modulates ischemia-damaged mitochondria during reperfusion. *J Cardiovasc Pharmacol* 2012;**59**:101–108.
41. Jennings RB. Historical perspective on the pathology of myocardial ischemia/reperfusion injury. *Circ Res* 2013;**113**:428–438.
42. Khan M, Cheema Y, Shahbaz A, Ahokas R, Sun Y, Gerling I, Bhattacharya SK, Weber KT. Mitochondria play a central role in nonischemic cardiomyocyte necrosis: common to acute and chronic stressor states. *Pflügers Arch* 2012;**464**:123–131.
43. Hoppel CL, Tandler B, Fujioka H, Riva A. Dynamic organization of mitochondria in human heart and in myocardial disease. *Int J Biochem Cell Biol* 2009;**41**:1949–1956.

44. Holmuhamedov EL, Oberlin A, Short K, Terzic A, Jahangir A. Cardiac subsarcolemmal and interfibrillar mitochondria display distinct responsiveness to protection by diazoxide. *PLoS One* 2012;**7**:e44667.
45. Kohr MJ, Aponte A, Sun J, Gucek M, Steenbergen C, Murphy E. Measurement of S-nitrosylation occupancy in the myocardium with cysteine-reactive tandem mass tags. *Circ Res* 2012;**111**:1308–1312.
46. Iwakiri Y, Satoh A, Chatterjee S, Toomre DK, Chalouni CM, Fulton D, Groszmann RJ, Shah VH, Sessa WC. Nitric oxide synthase generates nitric oxide locally to regulate compartmentalized protein S-nitrosylation and protein trafficking. *Proc Natl Acad Sci USA* 2006;**103**:19777–19782.
47. Maniatis NA, Brovkovych V, Allen SE, John TA, Shajahan AN, Tiruppathi C, Vogel SM, Skidgel RA, Malik AB, Minshall RD. Novel mechanism of endothelial nitric oxide synthase activation mediated by caveolae internalization in endothelial cells. *Circ Res* 2006;**99**:870–877.
48. Sanchez FA, Rana R, Kim DD, Iwahashi T, Zheng R, Lal BK, Gordon DM, Meininger CJ, Duran WN. Internalization of eNOS and NO delivery to subcellular targets determine agonist-induced hyperpermeability. *Proc Natl Acad Sci USA* 2009;**106**:6849–6853.
49. Ruiz-Meana M, Nunez E, Miro-Casas E, Martinez-Acedo P, Barba I, Rodriguez-Sinovas A, Inserte J, Fernandez-Sanz C, Hernando V, Vazquez J, Garcia-Dorado D. Ischemic preconditioning protects cardiomyocyte mitochondria through mechanisms independent of cytosol. *J Mol Cell Cardiol* 2014;**68**:79–88.
50. Wang S-B, Foster DB, Rucker J, O'Rourke B, Kass DA, Van Eyk JE. Redox regulation of mitochondrial ATP synthase: implications for cardiac resynchronization therapy. *Circ Res* 2011;**109**:750–757.